Brownian dynamics algorithm for bead-rod semiflexible chain with anisotropic friction

Alberto Montesi
Department of Chemical Engineering, Rice University, Houston, Texas 77005

David C. Morse
Department of Chemical Engineering and Material Science, University of Minnesota, Minneapolis, Minnesota 55455

Matteo Pasquali[a)]
Department of Chemical Engineering, Rice University, Houston, Texas 77005

(Received 17 August 2004; accepted 19 November 2004; published online 15 February 2005)

A model of semiflexible bead-rod chain with anisotropic friction can mimic closely the hydrodynamics of a slender filament. We present an efficient algorithm for Brownian dynamics simulations of this model with configuration dependent anisotropic bead friction coefficients. The algorithm is an extension of that given previously for the case of configuration independent isotropic friction coefficients by Grassia and Hinch [J. Fluid Mech. **308**, 255 (1996)]. We confirm that the algorithm yields predicted values for various equilibrium properties. We also present a stochastic algorithm for evaluation of the stress tensor, and we show that in the limit of stiff chains the algorithm recovers the results of Kirkwood and Plock [J. Chem. Phys. **24**, 665 (1956)] for rigid rods with hydrodynamic interactions. © *2005 American Institute of Physics*. [DOI: 10.1063/1.1848511]

I. INTRODUCTION

The dynamics of polymers in solution are often well described by Brownian dynamics simulations of models with geometrical constraints. Constraints may be introduced either in atomistic models, to represent fixed bond lengths or dihedral angles, or in more mesoscopic models of polymers as rigid rods, freely jointed bead-rod chains, or—considered here—longitudinally inextensible wormlike chains.

The design of a correct Brownian dynamics simulation of a model with constraints is not entirely trivial.[1] There are some subtle aspects of the equilibrium statistical mechanics of constrained models, which have been discussed for many years.[2–4] Additional, separate subtleties arise in the formulation of either stochastic differential equations or simulation algorithms for the Brownian motion of constrained systems,[1,5–9] most of which are common to any model of Brownian motion in which the diffusivity tensor depends upon the system configuration. Grassia and Hinch[10] have given an algorithm for the simulation of free-draining bead-rod polymers with constrained rod lengths and isotropic bead friction coefficients, which uses a midstep algorithm and a corrective pseudoforce that were both proposed by Fixman.[5] The simple case of a free-draining model with isotropic bead friction coefficients lends itself to mathematical simplifications that are not valid for models in which the friction tensor or diffusivity depends upon the polymer conformation, including the case considered here.

Accurate description of the dynamics of flexible polymers in dilute solution requires the use of a model with hydrodynamic interactions. In the limit of nearly straight, slender filaments, however, the effect of hydrodynamic screening may be accurately mimicked by a free draining model with an anisotropic effective friction coefficient tensor, in which the coefficient of friction for motion parallel to the polymer backbone is half of the coefficient for transverse motion.[11,12] The dynamics of many stiff polymers and filaments in dilute and semidilute solutions, including biopolymers (such as short DNA, collagen fibrils, rodlike viruses, F-actin, and xanthan), synthetic polymers [such as Poly(-benzyl-L-glutamate) (PBLG) and Poly(-p-phenylene-benzobisthiazole) (PBZT), used in the production of fibers], and single-walled carbon nanotubes, can be well described using the resulting slender body hydrodynamic approximation. Moreover, anisotropic friction has been used in some attempts to mimic the snakelike motion of a polymer in an entangled fluid,[4] and is needed to describe motion of a molecule in a liquid crystalline phase. In this paper, we consider a discretized model of semiflexible polymers with a local but anisotropic bead friction, with arbitrary perpendicular and parallel friction coefficients, which reduces to the slender body hydrodynamic approximation as a special case.

II. GENERIC MIDSTEP ALGORITHM

We use a midstep algorithm for constrained systems that was originally proposed by Fixman,[5] whose analysis has since been clarified and generalized by Hinch and Grassia[8–10] and Morse;[1] the prescription for simulating the Brownian motion of a generic constrained system of point particles is summarized here.

Consider a molecule of N beads with positions $\mathbf{R}_1, \ldots, \mathbf{R}_N$ that satisfy K constraints

[a)]Electronic mail: mp@rice.edu

$$C_\mu(\mathbf{R}_1, \ldots, \mathbf{R}_N) = \text{const} \quad \text{for } \mu = 1, \ldots, K. \tag{1}$$

The polymer is described by an inertialess Langevin equation for motion in a flow with a uniform velocity gradient $\boldsymbol{\kappa} = (\boldsymbol{\nabla v})^T$,

$$\boldsymbol{\zeta}_{ij} \cdot (\dot{\mathbf{R}}_i - \boldsymbol{\kappa} \cdot \mathbf{R}_i) = -\frac{\partial U}{\partial \mathbf{R}_j} - \mathbf{n}_{j\mu}\lambda_\mu + \boldsymbol{\eta}_j, \tag{2}$$

where $U(\mathbf{R}_1, \ldots, \mathbf{R}_N)$ is a potential energy, $\boldsymbol{\eta}_j$ is a random Langevin force, $\boldsymbol{\zeta}_{ij}$ is a friction tensor, which may depend on all bead positions, λ_μ is a constraint force conjugate to constraint μ, and

$$\mathbf{n}_{j\mu} \equiv \frac{\partial C_\mu}{\partial \mathbf{R}_j}. \tag{3}$$

Summation over repeated indices is implied *only* throughout this section. Defining a mobility tensor $\mathbf{H}_{ij}$, such that $\mathbf{H}_{ik} \cdot \boldsymbol{\zeta}_{kj} = \mathbf{I}\delta_{ij}$, leads to the equivalent form

$$\dot{\mathbf{R}}_i = \mathbf{H}_{ij} \cdot [\mathbf{F}_j^{\text{uc}} - \mathbf{n}_{j\mu}\lambda_\mu], \tag{4}$$

where

$$\mathbf{F}_j^{\text{uc}} = -\frac{\partial U}{\partial \mathbf{R}_j} + \mathbf{F}_j^{\text{f}} + \boldsymbol{\eta}_j \tag{5}$$

is the unconstrained force on bead j, and $\mathbf{F}_j^{\text{f}} = \boldsymbol{\zeta}_{ij} \cdot \boldsymbol{\kappa} \cdot \mathbf{R}_j$ is a "flow" force arising from the macroscopic velocity gradient.

If we treat the Langevin equation as an ordinary differential equation (ignoring for the moment any subtleties that arise because the resulting particle trajectories are actually not differentiable functions of time), the instantaneous values of the constraint forces $\lambda_1, \ldots, \lambda_K$ can be determined by requiring that

$$0 = \dot{C}_\mu = \mathbf{n}_{i\mu} \cdot \dot{\mathbf{R}}_i \quad \text{for } \mu = 1, \ldots, K \tag{6}$$

at each instant of time. This yields the set of linear equations

$$\hat{H}_{\mu\nu}\lambda_\nu = \mathbf{n}_{i\mu} \cdot \mathbf{H}_{ij} \cdot \mathbf{F}_j^{\text{uc}}, \tag{7}$$

where

$$\hat{H}_{\mu\nu} \equiv \mathbf{n}_{i\mu} \cdot \mathbf{H}_{ij} \cdot \mathbf{n}_{j\nu}. \tag{8}$$

Substituting the resulting constraint forces into Eq. (4) yields the equation of motion

$$\dot{\mathbf{R}}_i = \mathbf{P}_{ij} \cdot \mathbf{H}_{jk} \cdot \mathbf{F}_k^{\text{uc}}, \tag{9}$$

where

$$\mathbf{P}_{ij} \equiv \mathbf{I}\delta_{ij} - \mathbf{H}_{ik} \cdot \mathbf{n}_{k\mu}\hat{H}^{-1}_{\mu\nu}\mathbf{n}_{j\nu} \tag{10}$$

is termed a dynamical projection operator by Morse.[1]

The algorithm proposed by Hinch and co-workers,[8–10] which we follow here, requires that the random forces in the equation of motion be what Morse[1] terms geometrically projected random forces. These forces must satisfy

$$0 = \boldsymbol{\eta}_i \cdot \mathbf{n}_{i\mu} \text{ for } \mu = 1, \ldots, K, \tag{11}$$

so that the $3N$ dimensional vector $\boldsymbol{\eta}_i$ of random forces is locally tangent to the $3N-K$ dimensional hypersurface to which the system is confined. In the algorithm of interest, forces are generated at the beginning of each time step of length Δt by first generating unprojected random forces $\boldsymbol{\eta}'_1, \ldots, \boldsymbol{\eta}'_N$, with a variance

$$\langle \boldsymbol{\eta}'_i \boldsymbol{\eta}'_j \rangle = \frac{2kT}{\Delta t}\boldsymbol{\zeta}_{ij} \tag{12}$$

and then by taking

$$\boldsymbol{\eta}_j = \boldsymbol{\eta}'_j - \mathbf{n}_{j\mu}\hat{\eta}_\mu, \tag{13}$$

where $\hat{\eta}_\mu$ is a "hard" component of the $3N$ dimensional unprojected random force vector along direction $\mathbf{n}_{j\mu}$. The hard components of the random forces are given by the solution of a set of linear equations

$$\hat{G}_{\mu\nu}\hat{\eta}_\nu = \mathbf{n}_{j\mu} \cdot \boldsymbol{\eta}'_j, \tag{14}$$

where

$$\hat{G}_{\mu\nu} \equiv \mathbf{n}_{i\mu} \cdot \mathbf{n}_{i\nu}. \tag{15}$$

This construction is equivalent to taking $\boldsymbol{\eta}_i = \tilde{\mathbf{P}}_{ij} \cdot \boldsymbol{\eta}'_j$, where

$$\tilde{\mathbf{P}}_{ij} \equiv \mathbf{I}\delta_{ij} - \mathbf{n}_{i\mu}\hat{G}^{-1}_{\mu\nu}\mathbf{n}_{j\nu} \tag{16}$$

is termed geometrical projection operator.[1]

Both Hinch[8] and Morse[1] found that a corrective pseudoforce

$$\mathbf{F}_j^{\text{ps}} = kT\frac{\partial}{\partial \mathbf{R}_j} \ln \det(\hat{G}) \tag{17}$$

must be added to the force $\mathbf{F}_j$ on the right-hand side of Eqs. (4) or (9) in the midstep algorithm with geometrically projected random forces in order to obtain the correct equilibrium distribution. Fixman[5] originally found the same pseudoforce without explicitly introducing the notion of a geometrically projected random forces, a discrepancy that Morse traced to an ambiguity in Fixman's use of differential geometry. In fact, an algorithm that uses unprojected random forces can be devised, but would require a pseudoforce given by a different and generally more complicated expression.[1]

A single time step of the proposed midstep algorithm involves the following substeps.

(i) Construct unprojected random forces that satisfy Eq. (12), using the friction tensor $\boldsymbol{\zeta}_{ij}(\mathbf{R}_1^{(0)}, \ldots, \mathbf{R}_N^{(0)})$ obtained at a set of initial bead positions $\mathbf{R}_1^{(0)}, \ldots, \mathbf{R}_N^{(0)}$.

(ii) Use Eqs. (13)–(15) to construct geometrically projected random forces, using values of $\mathbf{n}_{j\mu}$ and $\hat{G}_{i\nu}$ obtained at the initial bead positions.

(iii) Calculate midstep positions $\mathbf{R}_1^{(1/2)}, \ldots, \mathbf{R}_N^{(1/2)}$ given by

$$\mathbf{R}_i^{(1/2)} = \mathbf{R}_i^{(0)} + \mathbf{V}_i^{(0)}\Delta t/2, \tag{18}$$

where $\mathbf{V}_i^{(0)}$ is the initial velocity of bead i calculated by using values of the forces, mobility, and normal vectors at the initial bead positions in Eqs. (4), (7), and (8), while adding the metric pseudoforce [Eq. (17)] to $\mathbf{F}_j$.

(iv) Calculate updated bead positions $\mathbf{R}_1^{(1)}, \ldots, \mathbf{R}_N^{(1)}$,

$$\mathbf{R}_i^{(1)} = \mathbf{R}_i^{(0)} + \mathbf{V}_i^{(1/2)}\Delta t, \tag{19}$$

where $\mathbf{V}_i^{(1/2)}$ is calculated using the deterministic forces, mobility tensor, and normal vectors at the midstep positions in Eqs. (4)–(8), but using the same projected random forces used in step (iii).

Previous applications of this algorithm have all been restricted to free draining models in which each bead has an isotropic friction coefficient ζ.[10,13–16] Such models yield $\hat{H}_{\mu\nu}=\hat{G}_{\mu\nu}/\zeta$, a mobility tensor $\mathbf{H}_{ij}=\delta_{ij}\mathbf{I}/\zeta$ proportional to the $3N$ dimensional identity tensor, and identical dynamical and geometric projection operators $\mathbf{P}_{ij}\equiv\tilde{\mathbf{P}}_{ij}$. In this special case, the contribution of the random forces to the velocity can be calculated using unprojected random forces and the pseudoforce of Eq. (17) without changing the the result. To see why, note that the random forces generally make a contribution to the velocity $\mathbf{P}_{ij}\cdot\mathbf{H}_{jk}\cdot\tilde{\mathbf{P}}_{kl}\cdot\boldsymbol{\eta}'_l$, which simplifies to $\mathbf{P}_{ij}\cdot\mathbf{P}_{jl}\cdot\boldsymbol{\eta}'_l/\zeta=\mathbf{P}_{il}\cdot\boldsymbol{\eta}'_l/\zeta$ because $\mathbf{P}$ is idempotent, making geometrical projection of the random forces redundant. In the case of anisotropic drag considered here, the analysis requires that the random forces be geometrically projected in a separate step prior to the calculation of constraint forces.

III. BEAD-ROD CHAIN WITH ANISOTROPIC FRICTION

The general algorithm described above is applied here to a bead-rod model of a wormlike chain with an anisotropic local friction. We consider a chain of length $L=(N-1)a$ represented by N beads connected by $N-1$ rods of constrained length a,

$$C_\mu = |\mathbf{R}_{\mu+1} - \mathbf{R}_\mu| = a \quad \text{for } \mu = 1, \ldots, N-1. \tag{20}$$

Differentiating C_μ with respect to bead positions $\mathbf{R}_i$ yields a vector

$$\mathbf{n}_{i\mu} = \mathbf{u}_\mu(\delta_{i,\mu+1} - \delta_{i,\mu}) \tag{21}$$

in which $\mathbf{u}_\mu=(\mathbf{R}_{\mu+1}-\mathbf{R}_\mu)/a$ is a unit vector parallel to bond μ. Equation (4) yields an equation of motion of the form

$$\dot{\mathbf{R}}_i = \mathbf{H}_{ij}\cdot\mathbf{F}_j^{\mathrm{tot}} \tag{22}$$

in which $\mathbf{H}_{ij}$ is the mobility of bead i in response to a force on bead j (for which a simple local approximation is introduced below), and

$$\mathbf{F}_j^{\mathrm{tot}} = \mathbf{F}_j^{\mathrm{uc}} + \lambda_j\mathbf{u}_j - \lambda_{j-1}\mathbf{u}_{j-1} \tag{23}$$

is the total force on bead j, including the contribution of the tensions in neighboring bonds, where λ_j is the tension in bond j. The unconstrained force is a sum

$$\mathbf{F}_i^{\mathrm{uc}} = -\frac{\partial U}{\partial \mathbf{R}_i} + \mathbf{F}_i^{\mathrm{ps}} + \mathbf{F}_i^{\mathrm{f}} + \boldsymbol{\eta}_i \tag{24}$$

that includes the metric, flow, and geometrically projected random forces. In the wormlike chain model, U is a bending potential, as discussed below.

The (anisotropic) mobility is $\mathbf{H}_{ij}=\delta_{ij}\boldsymbol{\zeta}_i^{-1}$, where $\boldsymbol{\zeta}_i^{-1}$ is an inverse bead friction tensor

$$\boldsymbol{\zeta}_i^{-1} = \frac{1}{\zeta_\parallel}\tilde{\mathbf{u}}_i\tilde{\mathbf{u}}_i + \frac{1}{\zeta_\perp}(\mathbf{I} - \tilde{\mathbf{u}}_i\tilde{\mathbf{u}}_i), \tag{25}$$

where $\zeta_\parallel=a\zeta_\parallel^*$ and $\zeta_\perp=a\zeta_\perp^*$ are bead friction coefficients and $\zeta_\parallel^*$ and $\zeta_\perp^*$ are the friction coefficients for motion, respectively, parallel and perpendicular to a local tangent vector $\tilde{\mathbf{u}}_i$. A slender filament in a viscous Newtonian liquid has

$$\zeta_\perp^* = 4\pi\eta_s\epsilon\left(\frac{1+0.64\epsilon}{1-1.15\epsilon} + 1.659\epsilon^2\right), \tag{26}$$

where $\epsilon\equiv\ln(L/r)$ and r is the filament hydrodynamic radius.[11,17] With this (local) choice of friction tensor, the velocity of each bead is related to the force on that bead alone, which yields an equation of motion

$$\dot{\mathbf{R}}_i = \boldsymbol{\zeta}_i^{-1}\cdot(\mathbf{F}_i^{\mathrm{uc}} + \lambda_i\mathbf{u}_i - \lambda_{i-1}\mathbf{u}_{i-1}). \tag{27}$$

The tangent $\tilde{\mathbf{u}}_i$ at bead i of a discretized chain is

$$\tilde{\mathbf{u}}_i = (\mathbf{u}_i + \mathbf{u}_{i-1})/|\mathbf{u}_i + \mathbf{u}_{i-1}|, \tag{28}$$

for $2\leqslant i\leqslant N-1$, and $\tilde{\mathbf{u}}_1=\mathbf{u}_1$ and $\tilde{\mathbf{u}}_N=\mathbf{u}_{N-1}$ at the chain ends.

The tensions can be obtained by requiring that $\dot{C}_\mu=0$ for all bonds, i.e., by solving a system of linear equations

$$\sum_{\nu=1}^{N-1}\hat{H}_{\mu\nu}\lambda_\nu = \mathbf{u}_\mu\cdot(\boldsymbol{\zeta}_{\mu+1}^{-1}\cdot\mathbf{F}_{\mu+1}^{\mathrm{uc}} - \boldsymbol{\zeta}_\mu^{-1}\cdot\mathbf{F}_\mu^{\mathrm{uc}}) \equiv Q_\mu \tag{29}$$

where $\mu=1,\ldots,N-1$ and

$$\hat{H}_{\mu\nu} = \sum_{i=1}^{N}\mathbf{n}_{i\mu}\cdot\boldsymbol{\zeta}_i^{-1}\cdot\mathbf{n}_{i\nu}, \tag{30}$$

or, in matrix form,

$$\hat{\mathbf{H}}\boldsymbol{\lambda} = \mathbf{Q}, \tag{31}$$

where $\hat{\mathbf{H}}$ is symmetric, positive definite, and tridiagonal

$$\hat{\mathbf{H}} = \begin{bmatrix} b_1 & a_2 & 0 & & \ddots & \\ a_2 & b_2 & a_3 & 0 & \ddots & \\ 0 & a_3 & \ddots & \ddots & 0 & \cdots \\ \ddots & 0 & \ddots & b_{N-3} & a_{N-2} & 0 \\ & \ddots & 0 & a_{N-2} & b_{N-2} & a_{N-1} \\ & & \ddots & 0 & a_{N-1} & b_{N-1} \end{bmatrix} \tag{32}$$

with diagonal elements

$$b_\mu = \frac{2}{\zeta_\perp} + \left(\frac{1}{\zeta_\parallel} - \frac{1}{\zeta_\perp}\right)[(\tilde{\mathbf{u}}_\mu\cdot\mathbf{u}_\mu)^2 + (\tilde{\mathbf{u}}_{\mu+1}\cdot\mathbf{u}_\mu)^2] \tag{33}$$

and off-diagonal elements

$$a_\mu = -\frac{1}{\zeta_\perp}\mathbf{u}_{\mu+1}\cdot\mathbf{u}_\mu - \left(\frac{1}{\zeta_\parallel} - \frac{1}{\zeta_\perp}\right)[(\tilde{\mathbf{u}}_\mu\cdot\mathbf{u}_{\mu+1})(\tilde{\mathbf{u}}_\mu\cdot\mathbf{u}_\mu)]. \tag{34}$$

Because $\hat{\mathbf{H}}$ is tridiagonal, the constraint forces can be calculated in $O(N)$ operations. Equation set (29) satisfies the length constraints to an accuracy of order Δt^2, as the original algorithm of Grassia and Hinch;[10] when the rod lengths deviate by more than a given tolerance (usually 10^{-3}), they are restored to a through a simple rescaling procedure. An accuracy of order Δt or higher for the average displacement of a

bead $\langle \Delta \mathbf{R}_i \rangle$ is required to obtain the correct drift term in the Fokker–Planck equation for the evolution of the probability distribution in the limit of $\Delta t \to 0$,[1] so that the order Δt^2 error in the constraints does not affect the limiting behavior of the algorithm (see Sec. VI for an estimate of the weak order of convergence of the complete algorithm).

The bending energy U of a discrete wormlike chain with bending rigidity κ is

$$U = -\frac{\kappa}{a}\sum_{k=2}^{N-1} \mathbf{u}_k \cdot \mathbf{u}_{k-1}. \tag{35}$$

Pasquali and Morse[15] have shown that the bending and metric forces can be obtained simultaneously, as a sum

$$\mathbf{F}_i^{\mathrm{b}} + \mathbf{F}_i^{\mathrm{ps}} = \frac{1}{a}\sum_{k=2}^{N-1} \kappa_k^{\mathrm{eff}} \frac{\partial(\mathbf{u}_k \cdot \mathbf{u}_{k-1})}{\partial \mathbf{R}_i}, \tag{36}$$

where

$$\kappa_i^{\mathrm{eff}} \equiv \kappa + k_B T a \hat{G}^{-1}_{i-1,i} \tag{37}$$

is a configuration-dependent effective rigidity, and that the matrix elements $\hat{G}^{-1}_{i-1,i}$ for $i=2,\ldots,N-1$ can be calculated in $O(N)$ operations by a fast recursion relation. The flow force is

$$\mathbf{F}_i^{\mathrm{f}} = \zeta_\perp \boldsymbol{\kappa} \cdot \mathbf{R}_i + (\zeta_\parallel - \zeta_\perp)\tilde{\mathbf{u}}_i(\tilde{\mathbf{u}}_i \cdot \boldsymbol{\kappa} \cdot \mathbf{R}_i) \tag{38}$$

for any model with the anisotropic bead mobility of Eq. (25).

Unprojected random forces are constructed by taking

$$\boldsymbol{\eta}_i' = \sqrt{24 k_B T}\, \boldsymbol{\zeta}_i^{1/2} \cdot \boldsymbol{\xi}_i \tag{39}$$

$$= \sqrt{24 k_B T}[\zeta_\perp^{1/2}\boldsymbol{\xi} + (\zeta_\parallel^{1/2} - \zeta_\perp^{1/2})\tilde{\mathbf{u}}_i\tilde{\mathbf{u}}_i \cdot \boldsymbol{\xi}_i], \tag{40}$$

where $\boldsymbol{\xi}_i = (\xi_{i1}, \xi_{i2}, \xi_{i3})$ are uncorrelated random vectors whose components ξ_{ia} are uniformly distributed random numbers between -0.5 and 0.5 with vanishing mean and variance $\langle \xi_{ia}^2 \rangle = 1/12$.

The algorithm for a chain with anisotropic friction requires that the unprojected random forces should be projected geometrically in a separate calculation. The projected mobility tensor $\hat{H}_{\mu\nu}$ (which involves the anisotropic friction tensors) and the projected metric tensor $\hat{G}_{\mu\nu}$ (which is a purely geometrical object) must be distinguished. Equation (13) for the hard components of the unprojected random forces can be expressed for a bead-rod chain as a set of $N-1$ linear equations:

$$\sum_{\nu=1}^{N-1} \hat{G}_{\mu\nu}\hat{\eta}_\nu = (\boldsymbol{\eta}_{\mu+1}' - \boldsymbol{\eta}_\mu') \cdot \mathbf{u}_\mu = P_\mu \tag{41}$$

or, in matrix notation,

$$\hat{\mathbf{G}}\hat{\boldsymbol{\eta}} = \mathbf{P}, \tag{42}$$

where $\hat{\mathbf{G}}$ is a symmetric, positive definite, and tridiagonal matrix with diagonal terms $G_{\mu\mu}=2$, and off-diagonal terms $G_{\mu,\mu-1} = -\mathbf{u}_\mu \cdot \mathbf{u}_{\mu-1}$. Therefore, the geometrically projected random forces are

$$\boldsymbol{\eta}_i = \boldsymbol{\eta}_i' + \hat{\eta}_{i+1}\mathbf{u}_{i+1} - \hat{\eta}_i \mathbf{u}_i. \tag{43}$$

In summary, the four steps outlined at the end of Sec. II are as follows.

(i) *Construct unprojected random forces*: Use Eq. (40), using bead friction tensors evaluated in the initial conformation.

(ii) *Geometrically project random forces*: Solve Eqs. (42) and (43), using $\tilde{\mathbf{u}}_i$ and $\hat{\mathbf{G}}$ evaluated in the initial conformation.

(iii) *Calculate midstep positions*: Add the deterministic bending, metric and flow forces to the geometrically projected random forces to obtain an $\mathbf{F}^{\mathrm{uc},(0)}$; use Eq. (31) to calculate the corresponding tensions $\lambda_\mu^{(0)}$, and evaluate the midstep bead positions

$$\mathbf{R}_i^{(1/2)} = \mathbf{R}_i^{(0)} + \frac{\Delta t}{2}\boldsymbol{\zeta}_i^{-1,(0)} \cdot \mathbf{F}_i^{\mathrm{tot},(0)}, \tag{44}$$

where $\mathbf{F}_i^{\mathrm{tot},(0)} = \mathbf{F}_i^{\mathrm{uc},(0)} + \lambda_{i+1}^{(0)}\mathbf{u}_{i+1}^{(0)} - \lambda_i^{(0)}\mathbf{u}_i^{(0)}$.

(iv) *Calculate updated positions*: Recalculate the unconstrained deterministic forces and total tensions at the midstep conformation to obtain the updated positions

$$\mathbf{R}_i^{(1)} = \mathbf{R}_i^{(0)} + \Delta t \boldsymbol{\zeta}_i^{-1,(1/2)} \cdot \mathbf{F}_i^{\mathrm{tot},(1/2)}. \tag{45}$$

IV. EVALUATION OF STRESS

To evaluate the stress tensor, we start from Kramers formula

$$\boldsymbol{\sigma} = -\sum_{i=1}^{N} \langle \mathbf{R}_i \mathbf{F}_i^{\mathrm{nh}} \rangle, \tag{46}$$

where

$$\mathbf{F}_i^{\mathrm{nh}} = \mathbf{F}_i^{\mathrm{tot}} - \mathbf{F}_i^{\mathrm{f}} \tag{47}$$

is the total nonhydrodynamic force (including the metric pseudoforce) acting on the bead i, which excludes the flow force $\mathbf{F}_i^{\mathrm{f}}$, but includes contributions to the tension that are induced by $\mathbf{F}_i^{\mathrm{f}}$. It has been shown[1] that the correct stress for the midstep algorithm used here is obtained by interpreting Eq. (46) as an average

$$\boldsymbol{\sigma} = -\frac{1}{2}\sum_{i=1}^{N} \langle \mathbf{R}_i^{(0)}\mathbf{F}_i^{\mathrm{nh},(0)} + \mathbf{R}_i^{(1)}\mathbf{F}_i^{\mathrm{nh},(1)} \rangle \tag{48}$$

of the virial tensor at beginning and end of the time step.

It is advantageous to divide the stress into components arising from smooth and random contributions to the unconstrained force $\mathbf{F}^{\mathrm{uc}}$, and to treat these contributions somewhat differently.[10] $\mathbf{F}^{\mathrm{uc}}$ is expressed as the sum of the random force $\boldsymbol{\eta}_i$ and a smooth component

$$\mathbf{F}_i^{\mathrm{smth}} \equiv \mathbf{F}_i^{\mathrm{b}} + \mathbf{F}_i^{\mathrm{m}} + \mathbf{F}_i^{\mathrm{f}}. \tag{49}$$

To simplify notation, it is convenient to define, for any force $\mathbf{F}_i$, a corresponding constrained force

$$\overline{\mathbf{F}}_i \equiv \sum_{j=1}^{N} \mathbf{F}_j \cdot \mathbf{P}_{ji} = \mathbf{F}_i + \tau_{i+1}\mathbf{u}_{i+1} - \tau_i \mathbf{u}_i, \tag{50}$$

where τ_i is the tension induced by $\mathbf{F}$, computed by solving

$$\sum_{\nu=1}^{N-1} \hat{H}_{\mu\nu}\tau_\nu = \mathbf{u}_\mu \cdot (\boldsymbol{\zeta}_{\mu+1}^{-1} \cdot \mathbf{F}_{\mu+1} - \boldsymbol{\zeta}_\mu^{-1} \cdot \mathbf{F}_\mu). \tag{51}$$

Using this notation, the total stress can be expressed as a sum of smooth and random components

$$\boldsymbol{\sigma}^{\mathrm{smth}} = -\sum_{i=1}^{N} \langle \mathbf{R}_i^{(0)} (\overline{\mathbf{F}}_i^{\mathrm{smth}} - \mathbf{F}_i^{\mathrm{f}})^{(0)} \rangle, \tag{52}$$

$$\boldsymbol{\sigma}^{\mathrm{rand}} = -\frac{1}{2}\sum_{i=1}^{N} \langle (\mathbf{R}_i^{(0)} \overline{\boldsymbol{\eta}}_i^{(0)}) + (\mathbf{R}_i^{(1)} \overline{\boldsymbol{\eta}}_i^{(1)}) \rangle. \tag{53}$$

In the above, we have used the fact that the Stratonovich-like interpretation of the time average used in Eq. (48) is necessary only for random stress components,[1] and that the correct value of $\boldsymbol{\sigma}^{\mathrm{smth}}$ is obtained in the limit $\Delta t \to 0$ by using values obtained at either the beginning (as above) or the end of a time step.

To evaluate the random stress, we use a technique introduced independently by Grassia and Hinch[10] and (in the context of a slightly different algorithm) by Doyle *et al.*[18] to filter out large but temporally uncorrelated fluctuations. Following these authors, we note that the stress contribution at the beginning of the time step, $\Sigma_{i=1}^{N} \langle \mathbf{R}_i^{(0)} \overline{\boldsymbol{\eta}}_i^{(0)} \rangle$ has zero mean but fluctuations of order $1/\sqrt{\Delta t}$. This term can be subtracted from the contribution at the end of the time step, without modifying the mean stress, while reducing its variance to order 1. The resulting filtered expression for the random stress is

$$\boldsymbol{\sigma}^{\mathrm{rand}} = -\frac{1}{2}\sum_{i=1}^{N} \langle \mathbf{R}_i^{(1)} \overline{\boldsymbol{\eta}}_i^{(1)} - \mathbf{R}_i^{(0)} \overline{\boldsymbol{\eta}}_i^{(0)} \rangle. \tag{54}$$

The total stress is then the sum of Eqs. (52) and (54).

V. VALIDATION

The above algorithm has been used to perform simulations of semiflexible chains in equilibrium and in steady shear flow. The anisotropy of the friction tensor affects the dynamics of the molecules, but chains with isotropic and anisotropic friction must satisfy the same theoretical Boltzmann distribution of conformations at equilibrium for the cosine of the angle between neighboring bond $\cos\theta_i = \mathbf{u}_i \cdot \mathbf{u}_{i-1}$:

$$P(\cos\theta_i) \propto e^{\kappa \cos\theta_i/(akT)}. \tag{55}$$

Results for this distribution are shown in Figs. 1 and 2 (top), for two different values of chain stiffness and a ratio $\zeta_\perp = 2\zeta_\parallel$. The results of the present algorithm, with geometrically projected random forces and a metric pseudoforce are compared with those of an incorrect algorithm that uses the same pseudo force but unprojected random forces. The correct algorithm yields results that agree with the predicted distribution to within statistical error, whereas the algorithm

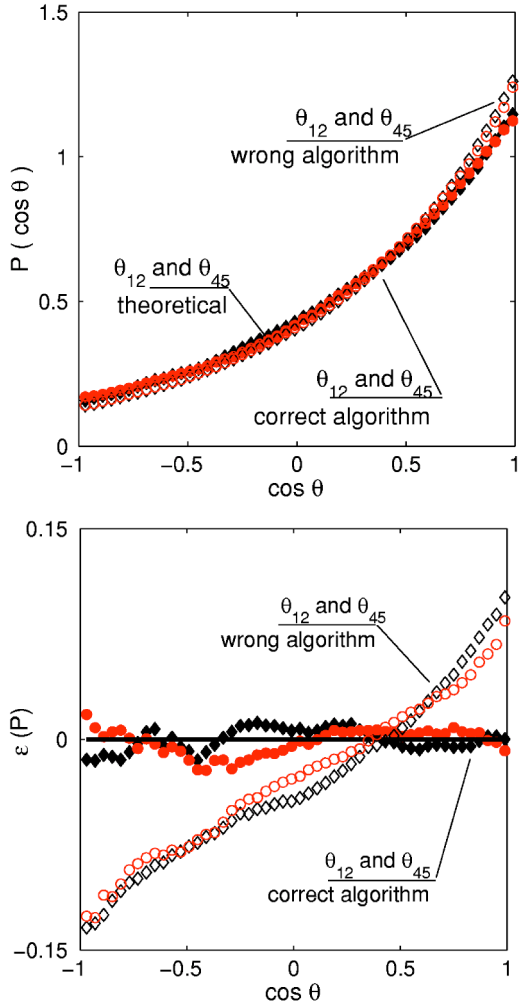

FIG. 1. Distribution of cosine of angles between rods 1 and 2 (○) and rods 4 and 5 (◇) in a chain of nine beads with anisotropic friction $\zeta_\parallel = 2\zeta_\perp$ for $\kappa/(akT) = 1$ or $L_p/L = 0.125$ (top) and relative error with respect to the theoretical distribution (bottom). The solid line denotes the normalized theoretical prediction $P(\cos\theta) = \exp[\kappa \cos\theta/(akT)]$. Solid symbols represent the correct algorithm and empty symbols represent the incorrect algorithm with unprojected noise. The symbols were computed by averaging the configuration of 400 molecules for ten times the rotational diffusion time of a rod of equal length. Initial configurations of the molecules were generated by sampling the theoretical distribution, then letting the system equilibrate for three rotational diffusion times before collecting data.

with unprojected forces clearly does not. The relative maximum error in the cosines distribution using the incorrect algorithm is about 15% for $\kappa/(akT) = 1$ [or $L_p/L = 0.125$, where $L_p \equiv \kappa/(kT)$ is the persistence length of the chain] and 10% for $\kappa/(akT) = 4$ (or $L_p/L = 0.5$). Of course, the relative error in the cosines distribution obtained with the incorrect algorithm vanishes in the isotropic limit and increases with increasing anisotropy. In simulations with $\zeta_\perp = 10\zeta_\parallel$, the maximum relative error is about 30% for $\kappa/(akT) = 1$ and 12% for $\kappa/(akT) = 4$. The relative error also diminishes for stiffer chains, because $\hat{\mathbf{H}} \to \hat{\mathbf{G}}/\zeta_\parallel$ as $\mathbf{u}_i \cdot \mathbf{u}_{i+1} \to 1$.

Results for the average stress tensor obtained in equilibrium simulations also agree with theoretical prediction. The stress tensor has zero off-diagonal terms (as a consequence of rotational isotropy) and diagonal terms of $-kT$ per polymer, corresponding to the ideal solution osmotic pressure of kT per polymer per unit volume.

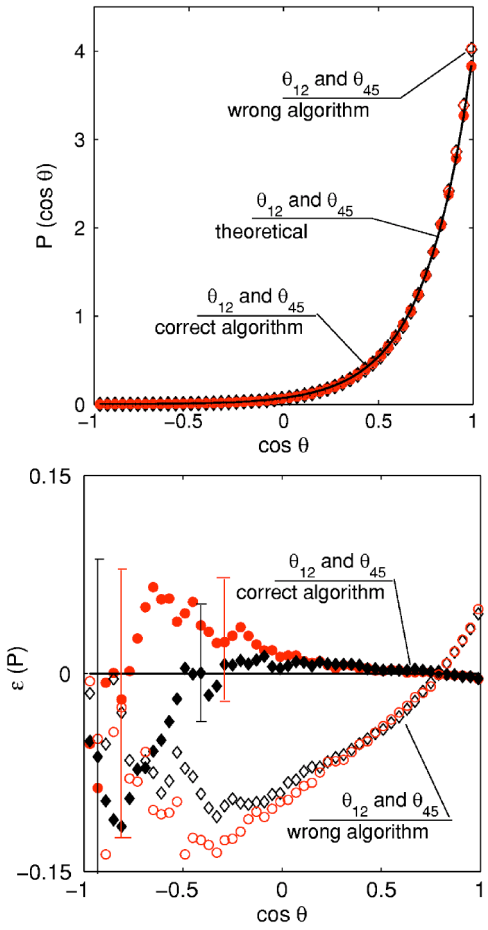

FIG. 2. Distribution of cosine of angles between rods 1 and 2 (○) and rods 4 and 5 (◇) in a chain of nine beads with anisotropic friction $\zeta_\parallel = 2\zeta_\perp$ for $\kappa/(akT) = 4$ or $L_p/L = 0.5$ (top) and relative error with respect to the theoretical distribution (bottom).

To validate the algorithm in presence of an external flow, simulations of very stiff wormlike chains with both $\zeta_\perp = 2\zeta_\parallel$ and $\zeta_\perp = \zeta_\parallel$ under steady shear have been conducted over a range of values of the shear rate $\kappa_{12} = \dot{\gamma}$, and compared to previous results for the steady shear viscosity of rigid rods with and without hydrodynamic interactions.

Although a closed-form expression for the viscosity as a function of the shear rate is not known, Kirkwood and Plock[19] calculated the shear viscosity of a dilute solution of rods, modeled as a line of Stokeslets with hydrodynamic interactions, by numerically solving the Smoluchowski equation for the distribution of rod orientations. In the limit of very large number of Stokeslets, i.e., for a rigid rod with hydrodynamic interactions, Kirkwood and Plock obtained a zero shear viscosity:

$$\eta_0^{\mathrm{rod}} = \tfrac{4}{5} kT \tau_{\mathrm{rod}} \nu, \tag{56}$$

where $\tau_{\mathrm{rod}} \equiv \zeta_\perp^* L^3/(72\ kT) = \tau_r$ is the rotational diffusion time of a rod and ν is the number of rods per unit volume. Kirkwood and Plock also found that the reduced shear viscosity η/η_0, where $\eta \equiv \boldsymbol{\sigma}_{12}/\dot{\gamma}$, decreases for values of the Weissenberg number $\mathrm{Wi} \equiv \dot{\gamma}\tau_r \gtrsim 0.1$, because the rods orient in the flow direction and therefore provide less viscous resistance; the slope of the shear thinning curve in presence of hydrodynamic interactions is equal to $-1/2$.[19]

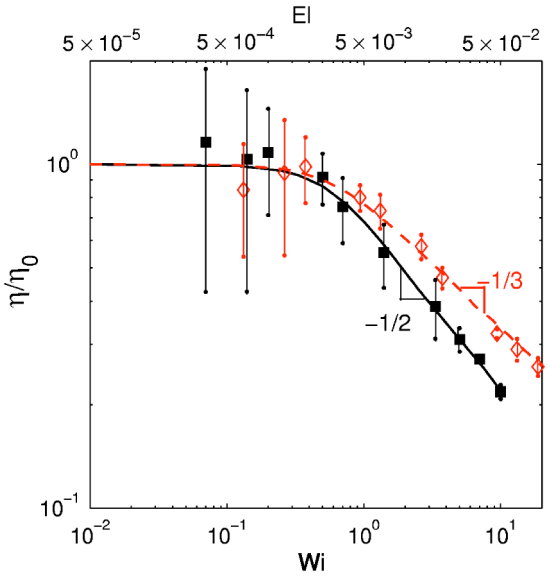

FIG. 3. Relative steady-shear viscosity (η/η_0) vs Weissenberg number $\mathrm{Wi} = \dot{\gamma}\tau_r$ reported by Kirkwood and Plock (Ref. 19) for rigid rods with hydrodynamics interactions (continuous line) and by Stewart and Sorensen (Ref. 24) for multibead rods without hydrodynamic interactions (dashed line), compared with the results of BD simulations for semiflexible rods with $L_p/L = 250$ and $\zeta_\perp/\zeta_\parallel = 2$ (rescaled with $\eta_0 = \eta_0^{\mathrm{rod}}$, $\tau_r = \tau_{\mathrm{rod}}$, ■) and $\zeta_\perp/\zeta_\parallel = 1$ (rescaled with $\eta_0 = \eta_0^{\mathrm{mb}}$, $\tau_r = \tau_{\mathrm{mb}}$, ◇).

To reproduce these results with our algorithm, we used semiflexible chains with $L_p/L = 250$, which are nearly straight, rodlike in equilibrium, and do not deform at the shear rates investigated here. Semiflexible chains can in fact deform in shear flow, undergoing a flow induced buckling instability;[20–23] such buckling however does not occur for small elasticity number, i.e., for $\mathrm{El} \equiv \dot{\gamma}\tau_b \ll 1$, where $\tau_b = \zeta_\perp^* (L/4.73)^4/\kappa$. In our simulations, $5 \times 10^{-5} \leqslant \mathrm{El} \leqslant 5 \times 10^{-2}$.

Figure 3 compares η/η_0 as a function of Wi from our simulations of stiff semiflexible chains with anisotropic friction to Kirkwood and Plock's results for rigid rods with hydrodynamic interactions. To compare the data, we take the rotational diffusion time for our model to be $\tau_r = \zeta_\perp a^2 (N-1)^3/(72\ kT)$; the results of our simulations agree with those of Kirkwood and Plock to within our statistical accuracy, thus validating both the simulation algorithm and the use of local anisotropic friction to mimic the hydrodynamics of rigid rods.

In Fig. 3 we also show the results obtained for the same stiff chains with isotropic friction. This results are compared with those of Stewart and Sorensen,[24] who have calculated the viscosity of a dilute solution of rigid dumbbells without hydrodynamic interactions, by numerically solving the corresponding diffusion equation in shear flow. Their results are also valid for multibead-rod models when the rigid dumbbell rotational diffusion time is replaced with the diffusion time for the multibead rod[4]

$$\tau_{\mathrm{mb}} \equiv \frac{\zeta L^2 N(N+1)}{72(N-1)kT} = \frac{\zeta a^2 (N-1)N(N+1)}{72kT} = \tau_{\mathrm{r}}. \qquad (57)$$

For this model, $\mathrm{Wi} = \dot{\gamma}\tau_{\mathrm{mb}}$ and $\eta_0^{\mathrm{mb}} = kT\tau_{\mathrm{mb}}\nu$. The agreement between our simulations and their numerical results is excellent.

VI. CONVERGENCE

We have investigated the convergence of our results with decreasing time step Δt by monitoring the dependence on Δt of the relative error for the average end-to-end distance $\langle R \rangle$, and for the distribution of values of the cosines of angles between consecutive bonds. Simulations have been performed with chains of nine beads with anisotropic friction $\zeta_{\parallel} = 2\zeta_{\perp}$ and $\kappa/(akT) = 1 (L_p/L = 0.125)$, and $\kappa/(akT) = 4 (L_p/L = 0.5)$. The errors have been computed by equilibrating 5000 chains for three times the rotational diffusion times for rods of equal length, then accumulating data for an additional ten rotational diffusion times.

The error on the distribution $P(\cos\theta)$ of values $\cos\theta$ of the angle θ between any two neighboring rods, which for this purpose is averaged over all seven pairs of neighboring rods, is defined as

$$\epsilon_{cos} = \int_{-1}^{1} |P(\cos\theta) - P_{eq}(\cos\theta)| P_{eq}(\cos\theta), \qquad (58)$$

where $P_{eq}(\cos\theta) = A \exp(\kappa \cos\theta/(akT))$ is the predicted distribution, and A is a normalization constant chosen such that $\int_{-1}^{1} d(\cos\theta) P_{eq}(\cos\theta) = 1$. The distribution $P(\cos\theta)$ is calculated numerically by dividing the interval $[-1,1]$ into 100 equal subintervals, and the error $\epsilon_{\cos}$ is obtained by approximating the above integral as a sum, and subtracting the integral of $P_{eq}(\cos\theta)$ over each subinterval from the simulated result for $P(\cos\theta)$.

The error on the average end to end distance is $\epsilon = |\langle R \rangle| - R_{eq}$, where R_{eq} is determined by an independent Monte Carlo simulation of 2×10^6 molecules.

Figure 4 presents the results of this convergence study. Both quantities show a linear convergence rate, i.e., $\epsilon \propto \Delta t$. This is the same order of global weak convergence (i.e., convergence of the probability distribution) as that found for a simple explicit Euler algorithm.[25]

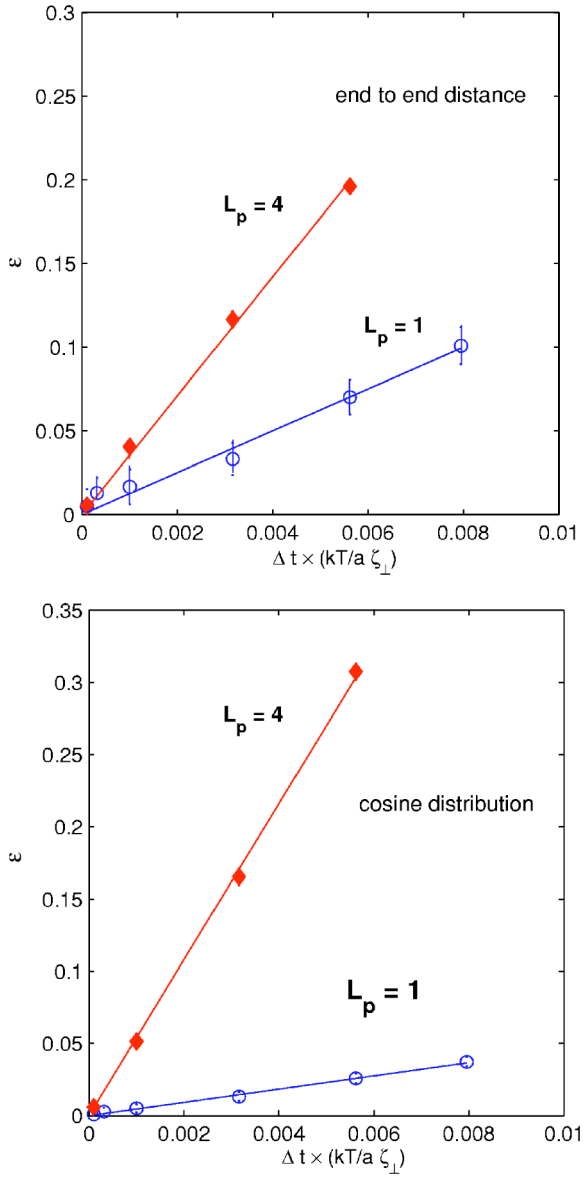

FIG. 4. Relative error vs Δt (symbols) and linear fit (lines) for the end to end distance (top) and for the cosine distribution (bottom) for chains with nine beads with anisotropic friction $\zeta_{\parallel} = 2\zeta_{\perp}$, $\kappa/(akT) = 1$ (○), and $\kappa/(akT) = 4$ (◆). The errors were computed averaging the configurations of 5000 chains for ten times τ_{rod}. Note that the error bars for $\epsilon_{\cos}$ are smaller than the symbols.

VII. EFFICIENCY

The computational cost per molecule for this algorithm scales linearly with N, with a prefactor only modestly larger than that found for the corresponding free-draining model with isotropic friction. In our implementation, tensions are computed by solving by fast LU factorization without pivoting[26] of the tridiagonal, symmetric, diagonally dominant matrices $\hat{\mathbf{G}}$ and $\hat{\mathbf{H}}$; uniformly distributed random numbers are generated with a Tausworthe long-period generator.[27] The algorithm was implemented in Fortran 90, compiled with Intel Compiler 8.0 and IBM XLF 7.1.0, and run on an Intel Pentium 4 2.8 GHz and an IBM Regatta with 1.3 GHz Power4 processors. A benchmark simulation of 10 000 steps for 100 semiflexible chains with 128 beads took 167.7 s on the Pentium and 151.7 s on the Regatta. On both machines, these times were ≈35% longer than the corresponding times (119.6 s and 113.7 s) for the same benchmark of an analogous code for semiflexible chains with isotropic friction. Most of the additional computational cost is due to the extra step of geometrically projecting the random forces in the case of anisotropic friction, which entails the solution of an additional tridiagonal system of $N-1$ linear equations once per time step.

VIII. DISCUSSION

The main result of this work is the design and implementation of a correct algorithm for Brownian dynamics simulations of constrained, semiflexible chains for which the friction coefficient $\boldsymbol{\zeta}_i$ of each bead is anisotropic and dependent

on the local chain conformation. A wormlike chain model with a ratio of friction coefficients $\zeta_\perp = 2\zeta_\parallel$ may be used to closely mimic the hydrodynamics of slender filaments.

The model studied here is perhaps the simplest physically relevant polymer model in which the friction tensor $\boldsymbol{\zeta}_{ij}$ depends upon the polymer conformation, as would also be true in any model with full hydrodynamic interactions. The midstep algorithm proposed by Fixman[5] has been found to require generally the use of geometrically projected random forces,[1,8,10] except in the case of free-draining chains with isotropic friction, in which $\boldsymbol{\zeta}_{ij} = \mathbf{I}\delta_{ij}\zeta$ is independent of chain conformation. Here, we confirm numerically that the use of geometrically projected random forces is necessary to obtain the desired equilibrium distribution in the case of interest.

The computational cost of the algorithm for semiflexible bead-rod chains with anisotropic friction coefficient is only slightly (i.e., about 35%) higher than of a corresponding model with isotropic friction, and much less than that expected for chains with full hydrodynamic interactions.

ACKNOWLEDGMENTS

This work was supported through Award No. CTS-CAREER-0134389, through the Nanoscale Science and Engineering Initiative under Award No. EEC-0118007, the Rice Terascale Cluster funded by NSF under Grant No. EIA-0216467, Intel and HP, and the Minnesota Supercomputing Institute.

[1] D. C. Morse, Adv. Chem. Phys. **128**, 65 (2004).
[2] H. Kramers, J. Chem. Phys. **14**, 415 (1946).
[3] M. Fixman, Proc. Natl. Acad. Sci. U.S.A. **74**, 3050 (1974).
[4] R. A. Bird, C. F. Curtiss, R. C. Armstrong, and O. Hassager, *Dynamics of Polymeric Liquids*, 2nd ed. (Wiley, New York, 1987), Vol. 2.
[5] M. Fixman, J. Chem. Phys. **69**, 1527 (1978).
[6] H.-C. Öttinger, Phys. Rev. E **50**, 2696 (1994).
[7] H.-C. Öttinger, *Stochastic Processes in Polymeric Fluids*, 1st ed. (Springer, Berlin, 1996).
[8] E. J. Hinch, J. Fluid Mech. **271**, 219 (1994).
[9] P. S. Grassia, E. J. Hinch, and L. C. Nitsche, J. Fluid Mech. **282**, 373 (1995).
[10] P. S. Grassia and E. J. Hinch, J. Fluid Mech. **308**, 255 (1996).
[11] G. K. Batchelor, J. Fluid Mech. **44**, 419 (1970).
[12] M. Doi and S. F. Edwards, *The Theory of Polymer Dynamics*, 1st ed. (Oxford University Press, Oxford, 1986).
[13] M. Pasquali, V. Shankar, and D. C. Morse, Phys. Rev. E **64**, 020802(R) (2001).
[14] P. Dimitrakopoulos, J. F. Brady, and Z. G. Wang, Phys. Rev. E **64**, 050803 (2001).
[15] M. Pasquali and D. C. Morse, J. Chem. Phys. **116**, 1834 (2002).
[16] P. Dimitrakopoulos, J. Chem. Phys. **119**, 8189 (2003).
[17] R. G. Larson, *The Structure and Rheology of Complex Fluids* (Oxford University Press, New York, 1999).
[18] P. S. Doyle, E. S. Q. Shaqfeh, and A. P. Gast, J. Fluid Mech. **334**, 251 (1997).
[19] J. G. Kirkwood and R. G. Plock, J. Chem. Phys. **24**, 665 (1956).
[20] O. L. Forgacs and S. G. Mason, J. Colloid Sci. **14**, 457 (1958).
[21] L. Becker and M. Shelley, Phys. Rev. Lett. **87**, 198301 (2001).
[22] C. H. Wiggins, A. Montesi, and M. Pasquali, e-print cond-mat/0307551 (2003).
[23] A. Montesi, C. H. Wiggins, and M. Pasquali (unpublished).
[24] W. E. Stewart and J. P. Sorensen, Trans. Soc. Rheol. **16**, 1 (1972).
[25] P. E. Kloeden, E. Platen, and H. Schurz, *Numerical Solution of Stochastic Differential Equations Through Computer Experiments* (Springer, New York, 1997).
[26] J. J. Lambiotte and R. G. Voigt, ACM Trans. Math. Softw. **1**, 308 (1975).
[27] P. L'Ecuyer, Math. Comput. **65**, 203 (1996).